

Magnesium Dicyanide: Three Isomers or Seven?

Simon Petrie*

Research School of Chemistry, Australian National University, Canberra, A. C. T. 0200, Australia

Received: August 18, 1998

We present a detailed study of the singlet potential energy surface for $\text{Mg}(\text{CN})_2$ using a variety of ab initio computational techniques. When second-order Møller–Plesset perturbation theory is employed in conjunction with basis sets of various sizes, seven structures for $\text{Mg}(\text{CN})_2$ are identified as local minima: the linear isomers NCMgCN , NCMgNC , and CNMgNC and the π -complex species $\text{NCMg}-\pi(\text{CN})$, $\text{CNMg}-\pi(\text{CN})$, and $\text{Mg}[-\pi(\text{CN})]_2$ (two enantiomers). These isomers are connected by eight transition states to isomerization. However, while the linear structures are also found to be minima at all of the levels of theory employed here, the existence of the π -complexes (and, consequently, of many of the transition states) is strongly level-dependent: at B3-LYP/6-31+G*, B3-LYP/6-311+G(2df), and with Hartree–Fock calculations with a variety of basis sets, none of the π -complexes correspond to stationary points upon the potential energy surface. Furthermore, calculations employing methods designed to deliver highly accurate molecular energies (such as G2 and CBS-Q) reveal that the π -complexes located on the MP2/6-31G* surface are higher in energy than some of the putative transition states leading to linear isomers. While a more detailed examination of partially optimized structures upon the potential energy surface (using various levels of theory including QCISD/6-311G(2df), G2, and CBS-Q, with B3-LYP/6-311+G(2df) geometries) suggests that the π -complexes are, technically, local minima, we conclude that these π -complexes are, at best, highly reactive intermediates on the isomerization pathways $\text{NCMgCN} \leftrightarrow \text{NCMgNC}$ and $\text{NCMgNC} \leftrightarrow \text{CNMgNC}$ and that only the linear minima (NCMgCN , NCMgNC , and CNMgNC) correspond to meaningful and isolable chemical entities. According to both the G2 and CBS-Q techniques, the difference between the highest transition state and the global minimum (CNMgNC) is only $\sim 30 \text{ kJ mol}^{-1}$.

Introduction

One of the fundamental differences between strong ionic and covalent bonds of comparable strength is that an ionic bond between a metal cation and a molecular anion may be almost completely lacking in the directional dependence expected for a covalent interaction. A striking example of this phenomenon is that, whereas covalent HCN is separated from its considerably higher energy isomer HNC by a barrier of $\sim 180 \text{ kJ mol}^{-1}$ (corresponding to $\sim 35\%$ of the energy required for the dissociation $\text{HCN} \rightarrow \text{H} + \text{CN}$),¹ the isomerization pathway upon the $\text{Na}(\text{CN})$ potential energy surface is confined within a relative energy range of only $\sim 15 \text{ kJ mol}^{-1}$ (i.e., only $\sim 3.5\%$ of the $\text{Na}-\text{CN}$ dissociation energy).² Furthermore, the global minimum for the sodium cyanide molecule is a “T-shaped” π -complex, with both linear forms NaCN and NaNc constituting shallow local minima or second-order saddle points, depending upon the level of theory employed to study this potential energy surface.^{2,3}

The characterization of species such as $\text{Na}(\text{CN})$, which are variously described as “floppy”, nonrigid, or polytopic molecules,⁴ is important with regard to the insights offered by such studies into the largely electrostatic interaction between a metal atom and its ligand(s). The isomerism (or polytopism) of many metal cyanides, including the lithium,^{1f,2c–e,3,5} sodium,^{2,3} magnesium,^{2g,6} potassium,^{2b,e,4c,5f,7} and calcium^{6a,i,8} monocyanoanides, has been investigated both experimentally and by ab initio methods. A general trend evident in these studies has been that alkali metal monocyanoanides preferentially adopt a π -complex structure^{2,3,7} (although this does not hold true for the smallest

alkali metal, lithium)⁵ while the alkaline earth monocyanoanides are more prone to form a linear isocyanide MNC .^{6,8} In some instances, notably the cation $\text{Mg}(\text{CN})^+$,^{6f–h} all three geometries, linear MCN , linear MNC , and π -complex, are seen to be local minima according to high-level ab initio calculations, with comparatively small barriers to interconversion.

An even more extreme example of multiple isomerism for a metal cyanide compound has been provided recently by Kapp and Schleyer,⁹ who have located, using ab initio calculations, five discrete isomers of the compound magnesium dicyanide, $\text{Mg}(\text{CN})_2$. Kapp and Schleyer’s study,⁹ which addressed the issue of isomerism in alkaline earth dicyanoanides generally, employed geometry optimizations at the MP2/6-31+G* level and single-point total-energy calculations at MP4SDTQ(fc)/6-311+G(2d). Given the virtually flat potential energy surfaces typically associated with alkali metal and alkaline earth monocyanoanides, which require fairly high levels of theory to characterize correctly, it is unclear that the study of Kapp and Schleyer⁹ provides a definitive examination of the $\text{Mg}(\text{CN})_2$ potential energy surface. The present study attempts to redress this, through the location of all feasible transition states between $\text{Mg}(\text{CN})_2$ isomers, through the use of high-level ab initio techniques for calculations on the various stationary points, and through detailed explorations of the potential energy surface in the vicinity of certain putative minima and transition states.

Theoretical Methods

The present study uses a variety of computational techniques, all of which have been implemented using the Gaussian94

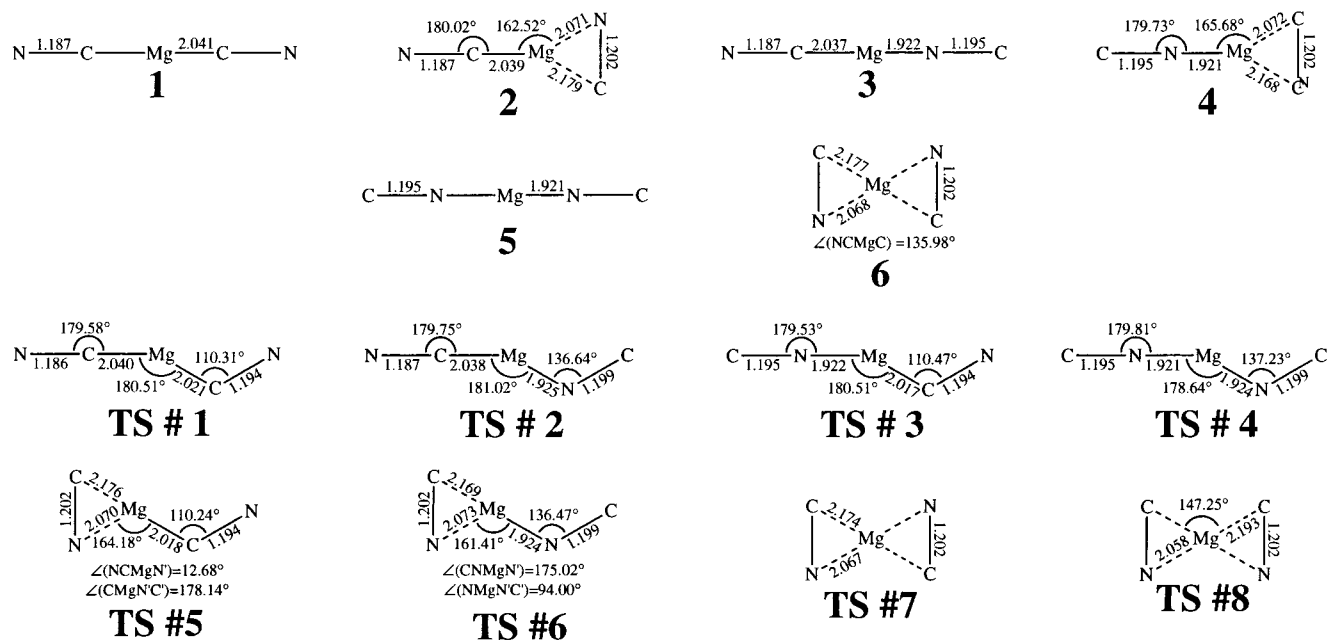


Figure 1. Optimized geometries of $\text{Mg}(\text{CN})_2$ stationary points, obtained at the MP2(full)/6-31G* level of theory.

programming package.¹⁰ Calculations at the Gaussian-2 (G2) level of theory have been undertaken in accordance with the established method as previously described,^{11,12} using either HF/6-31G*¹¹ or MP2(full)/6-31G*¹² (corrected) zero-point energies. Calculations using the CBS-Q technique have been executed either in the prescribed manner¹³ or, alternatively, using the same optimized geometries and ZPE corrections as implemented in the G2 calculations. The G2 and CBS-Q methods are complex “model chemistry” techniques that use a combination of single-point total-energy calculations to yield highly accurate thermochemical values; both methods typically perform to an accuracy of well within ± 10 kJ mol⁻¹.^{11,14,15} Further geometry optimizations and some single-point calculations were performed using various treatments for electron correlation, namely, second- and fourth-order Møller–Plesset perturbation theory, coupled-cluster (CC) and quadratic configuration interaction (QCI) techniques, both including single, double, and perturbative triple excitations; and the widely used hybrid density functional method B3-LYP. Basis sets employed in these calculations ranged from 6-31G-(d) to 6-311+G(3df), although the calculations involving the highest level of electron correlation (QCISD(T) and CCSD(T)) were not attempted using the largest of these basis sets.

Results and Discussion

Initial Geometry Optimizations. Geometry optimizations, at the HF/6-31G* and MP2(full)/6-31G* levels of theory, were performed as a component of the G2 calculations upon the $\text{Mg}(\text{CN})_2$ potential energy surface (PES), since both of these levels of theory are required to provide zero-point energy values and geometries for the subsequent single-point total-energy calculations of the standard G2 method. The results of the HF/6-31G* and MP2(full)/6-31G* calculations are, qualitatively, in very serious conflict; at both levels of theory, the PES is found to be rather flat, but the surface is apparently much more complex at MP2/6-31G* than is the case at HF/6-31G*. We detail the MP2 geometries in Figure 1, while the disparity between the HF and MP2 surfaces is well illustrated by the diagrams in Figures 2 and 3.

The MP2(full)/6-31G* structures parallel rather closely the geometries obtained with MP2/6-31+G*, as reported previously

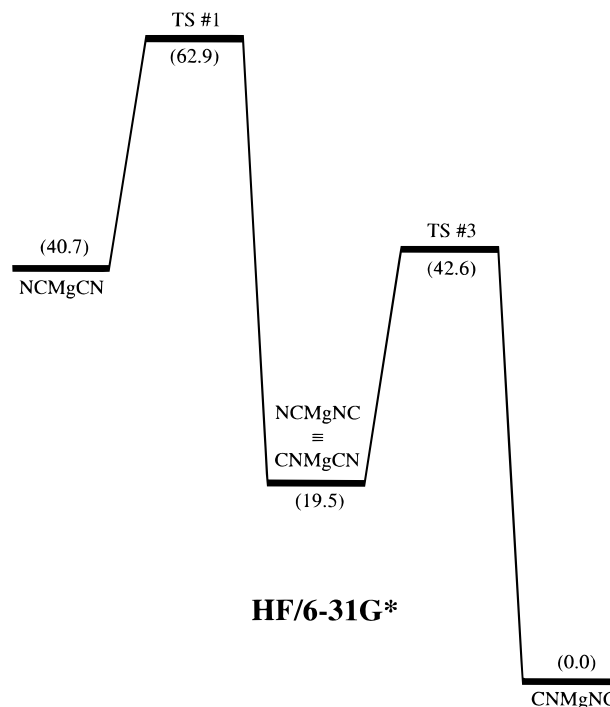


Figure 2. Schematic diagram of isomerization pathways located for $\text{Mg}(\text{CN})_2$ at the HF/6-31G* level of theory. Relative energies are given in kJ mol⁻¹.

by Kapp and Schleyer.⁹ However, the earlier study did not include the structure $\text{CNMgNC}-\pi(\text{CN})$ ¹⁶ and excluded also all transition states other than those between the two $\text{Mg}-\pi(\text{CN})_2$ enantiomers.

We may enumerate several significant differences between our HF and MP2 results. First, as noted above, the MP2 surface possesses many more minima and transition states than does the HF surface, with only linear species found to be minima at HF/6-31G*. Second, the diisocyanide CNMgNC is the global minimum at HF/6-31G*, whereas NCMgCN is the lowest-energy isomer according to the MP2/6-31G* calculations. Third, the transition state that corresponds to $\text{XMgCN} \leftrightarrow \text{XMgNC}$ isomerization according to the Hartree–Fock calculations is very

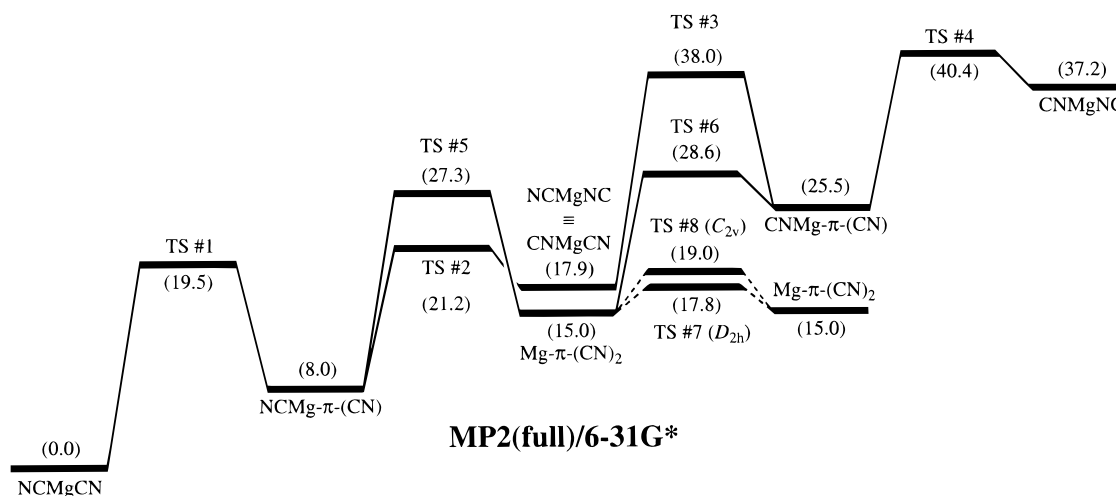


Figure 3. Schematic diagram of isomerization pathways located for $\text{Mg}(\text{CN})_2$ at the MP2(full)/6-31G* level of theory. Relative energies are given in kJ mol^{-1} .

TABLE 1: Total Energies, Enthalpies of Formation, and Relative Energies of $\text{Mg}(\text{CN})_2$ Isomers, Obtained at the G2 and CBS-Q Levels of Theory

species ^a	ZPE ^b	$n(i)^c$	G2			CBS-Q		
			E_0^d	$\Delta H_{f,0}^e$	E_{rel}^f	$E_0^{d,g}$	$\Delta H_{f,0}^e$	E_{rel}^f
NCMgCN (1) ($D_{\infty h}$)	14.63	0	-385.110 00	251.9	7.8	-385.113 66	252.8	15.2
TS #1 (1 ↔ 2) (C_s)	13.74	1	-385.102 69	271.1	27.0	-385.106 16	272.5	34.9
NCMg- π -(CN) (2) (C_s)	12.80	(0)	-385.109 85	252.3	8.2	-385.113 41	253.5	15.9
TS #2 (2 ↔ 3) (C_s)	12.82	(1)	-385.110 91	249.5	5.4	-385.115 56	247.8	10.2
NCMgNC (3) ($C_{\infty v}$)	14.11	0	-385.111 64	247.6	3.5	-385.116 63	245.0	7.4
TS #3 (3 ↔ 4) (C_s)	13.17	1	-385.104 19	267.1	23.1	-385.108 97	265.1	27.5
CNMg- π -(CN) (4) (C_s)	12.58	(0)	-385.110 93	249.4	5.4	-385.116 41	245.6	8.0
TS #4 (4 ↔ 5) (C_s)	12.46	(1)	-385.112 08	246.4	2.4	-385.118 44	240.3	2.7
CNMgNC (5) ($D_{\infty h}$)	13.56	0	-385.112 98	244.1	0.0	-385.119 44	237.6	0.0
TS #5 (2 ↔ 6) (C_1)	12.13	(1)	-385.109 26	253.8	9.7	-385.114 71	250.1	12.5
TS #6 (4 ↔ 6) (C_1)	12.12	(1)	-385.101 96	273.0	28.9	-385.105 99	273.0	35.4
$\text{Mg}[-\pi-(\text{CN})]_2$ (6) (C_{2v})	12.29	(0)	-385.107 94	257.3	13.2	-385.112 38	256.2	18.6
TS #7 (6 ↔ 6') (D_{2h})	12.02	(1)	-385.107 45	258.6	14.5	-385.111 99	257.2	19.6
TS #8 (6 ↔ 6') (C_{2v})	12.07	(1)	-385.119 74	258.0	13.9	-385.112 24	256.5	18.9

^a Species shown in italics are not stationary points on the HF/6-31G* potential energy surface. For such species, zero-point vibrational energy has been calculated at the MP2(full)/6-31G* level of theory (and adjusted by a scale factor of 0.9427);¹⁷ total energies for species in italics are thus obtained at the G2(ZPE = MP2)¹² or CBS-Q(ZPE = MP2) level of theory. All transition states are designated as, for example, (**2** ↔ **3**), according to the neighboring minima at MP2(full)/6-31G*. ^b Zero-point vibrational energy in mhartrees (1 mHartree = 2.6255 kJ mol^{-1}), obtained at the HF/6-31G* level of theory (corrected by a factor of 0.8929) unless otherwise indicated. ^c Number of imaginary frequencies obtained in the HF/6-31G* frequency calculation used to determine ZPE. Values in brackets are for the MP2(full)/6-31G* frequency calculation, where this yields a qualitatively different result. ^d Calculated total energy (in hartrees), including ZPE. ^e Calculated (0 K) enthalpy of formation, in kJ mol^{-1} . ^f Relative energy according to the indicated level of theory, in kJ mol^{-1} . ^g The version of CBS-Q employed for these calculations differs from the standard version.¹³ See text for details.

similar to the $\text{XMgCN} \leftrightarrow \text{XMg-}\pi\text{-(CN)}$ transition state at MP2; with the correlated method, direct interconversion of XMgCN and XMgNC is not possible.

Given the comparatively small basis set employed in these calculations and the apparent “low-contrast” nature of the potential energy surface at both levels of theory, the disagreement between these methods is not too surprising. In the absence of other information, we would most likely anticipate that the MP2 results, which include electron correlation, are inherently more reliable than the “single-electron” Hartree–Fock calculations. This expectation can usefully be assessed by further calculations at higher levels of theory, as discussed in the following sections.

G2 Calculations. The G2 total energies, obtained from the MP2/6-31G* geometries, are detailed in Table 1. The tabulated values include some anomalous results. Most obviously, the G2 total energies obtained for the various π -complexes $\text{XMg-}\pi\text{-(CN)}$ are *higher* than those for the respective transition states leading to the isocyanides XMgNC , a clear reversal of the

relative energies on the MP2(full)/6-31G* surface. A more subtle feature of the G2 results is that the relative energies of these geometries are dependent on the level of theory; while, according to G2, the transition state to formation of XMgNC possesses a lower total energy than $\text{XMg-}\pi\text{-(CN)}$, the reverse is true at virtually all of the lower levels of theory employed¹¹ in constructing the G2 total energy. This odd result, which holds largely true also for the relative energies of species XMgCN possessing a linear MgCN moiety and the corresponding isocyanides XMgNC , is illustrated by the relative energy values given in Table 2.

Given the apparent discrepancies in relative energy noted above, can G2 be relied upon to yield an accurate description of the potential energy surface? This is not a straightforward question to answer. G2 theory is normally held to be accurate to within $\pm 8 \text{ kJ mol}^{-1}$ for most species,^{11,14} and the energy differences being examined here are generally much smaller; however, the potential energy surface is rather “flat”, with the cyanide ligands’ orientation able to affect the $\text{CNMg-}\pi\text{-(CN)}$

TABLE 2: Relative Energies, between XMgCN and XMgNC Isomers and between XMg- π (CN) and Neighboring Transition States, at Various Levels of Theory

level	A: B:	NCMgNC NCMgCN	CNMgNC CNMgCN	ΔE_e (A - B) ^a (CN)- π -MgNC (CN)- π -MgCN	NCMg- π (CN) TS 2	CNMg- π (CN) TS 4
MP2/6-311G(d) ^b		+5.45	+5.73	+5.29	+3.35	+3.68
MP2/6-311+G(d)		+5.38	+5.47	+5.49	+2.63	+2.65
MP2/6-311G(2df)		+2.66	+2.79	+2.64	+1.33	+1.43
MP2/6-311+G(3df) ^b		+3.17	+3.25	+3.18	+1.00	+1.04
MP4/6-311G(d)		+2.05	+2.36	+1.95	+1.66	+1.95
MP4/6-311+G(d)		+1.96	+2.08	+2.15	+0.94	+0.90
MP4/6-311G(2df)		+0.10	+0.25	-0.21	-0.07	-0.02
QCISD(T)/6-311G(d) ^b		+0.68	+1.24	+0.76	+0.98	+1.35
G2(MP2)		-1.60	-1.24	-1.35	-1.37	-1.29
G2		-1.13	-0.79	-0.86	-1.08	-1.03

^a Energy difference between the stationary points A and B at the indicated level of theory, in mhartrees. Relative energies at all levels of theory are for the MP2(full)/6-31G* optimized geometries and do not include ZPE. ^b This level of theory is also employed in calculating a G2(MP2) total energy.

bond strength by less than 6%. Under these circumstances, we might expect the G2 relative energies for Mg(CN)₂ isomers to be rather more accurate than (for example) the G2 $\Delta H^\circ_{f,0}$ value for NCMgCN, and it is the latter property to which the expected accuracy of ± 8 kJ mol⁻¹ is more properly attached. Furthermore, while there is an evident conflict in Table 2 between the G2 relative energies and the relative energies obtained at G2's various "constituent" levels of theory, the conflict is, in all cases, by far the greatest when G2 is being contrasted with the lowest level of electron correlation (MP2, second-order Møller–Plesset perturbation theory) or with the smallest basis sets (6-311G(d) and 6-311+G(d)); the use of more sophisticated methods for electron correlation (full fourth-order Møller–Plesset perturbation theory (MP4) or quadratic configuration interaction with singles, doubles, and perturbative triples (QCISD(T)) or of a larger basis set (6-311G(2df) or 6-311+G(3df)) always reduces the disagreement with G2. This tendency provides some support to the reliability of the G2 relative energies.

In Table 2, we have also shown the relative energies, for pairs of stationary points, at the G2(MP2) level of theory. G2(MP2) is a less computationally expensive technique that attempts to emulate the same level of theory (QCISD(T) = fc/6-311+G(3df,2p)) as does G2, using a "subset" of the single-point calculations that comprise the G2 technique. Note that, in keeping with the trend for G2, G2(MP2) finds that the XMgNC geometry is preferred over the corresponding XMgCN isomer in all instances, while the opposite is true at each constituent level of theory. Similarly, the π -complex XMg- π (CN) is not a "true" minimum according to G2(MP2) since it lies above the energy of the associated transition state to isomerization to the corresponding isocyanide XMgNC, although again this is not reflected in the relative energies obtained at the various constituent levels of theory. The good agreement between G2 and G2(MP2) is encouraging and suggests that the two methods are of comparable reliability.

A further useful test of the G2 and G2(MP2) relative energies would be to calculate relative energies at the QCISD(T)/6-311+G(3df) level of theory [which is the "goal" of both G2 and G2(MP2)]; however, with our present computational resources, such calculations on these species are prohibitively demanding in CPU time and memory requirements. We have performed QCISD(T)/6-311+G(3df) calculations upon chemically similar, smaller systems such as Na(CN) and FMg(CN), and for all stationary points upon these "model" potential energy surfaces the agreement between G2 and the QCISD(T)/6-311+G(3df) calculations is excellent. Therefore, we can infer that the additivity assumptions (which imply that G2 can

satisfactorily reproduce the results of a QCISD(T)/6-311+G(3df) calculation) are very likely to hold well for the Mg(CN)₂ potential energy surface.

Two further methodological questions arise from our examination of the performance of G2 for this surface. First, is QCISD(T)/6-311+G(3df) a sufficiently high level of theory to characterize the Mg(CN)₂ surface to high accuracy if we wish to correctly assign relative energies for all of these low-lying isomers? Second, is MP2(full)/6-31G* an adequate level of theory with which to perform geometry optimizations if we wish to infer from subsequent single-point calculations whether the π -complexes are genuine minima or whether the isocyanide geometries are preferred over the corresponding cyanides? We shall address these questions in subsequent sections.

CBS Calculations. As one of several checks upon the validity of the G2 results, we have performed total-energy calculations using one of the "complete basis set" (CBS) methods of Peterson and co-workers.¹³ Our CBS-Q values for Mg(CN)₂ isomers, listed in Table 1, differ from the standard CBS-Q technique¹³ in that they employ MP2(full)/6-31G* geometries and HF/6-31G* (or MP2/6-31G*) zero-point energies rather than the MP2-(fc)/6-31G[†] geometries and HF/6-311G** ZPE values normally implemented in this technique; nevertheless, we do not expect that these modifications will affect the total energies thus obtained in any significant way. In any event, most of the stationary points that we report here cannot be located on the HF/6-311G** potential energy surface so that only a very restricted set of stationary points (effectively, those shown in Figure 2) can be treated by standard CBS-Q theory.¹⁸ The purpose of using the same methods for geometry optimization and for zero-point energy in both our G2 and CBS-Q calculations is to assist in a more transparent comparison of the two methods of basis set extrapolation with regard to the Mg(CN)₂ potential energy surface.

The agreement between our G2 and CBS-Q values is excellent; all of the findings of our G2 investigation are supported by the CBS-Q results. Thus, for both methods, the ordering of linear isomers (from most to least stable) is found to be CNMgNC, NCMgNC, NCMgCN; the π -complex geometries NCMg- π (CN), CNMg- π (CN), and Mg- π (CN)₂ are also found to be unstable with respect to the geometries of the putative transition states TS 2, TS 4, and TS 5, respectively. There are, nevertheless, small quantitative differences between the two techniques; the stabilization of the isocyanide geometry XMgNC relative to XMgCN is greater for CBS-Q (~ 7.6 kJ mol⁻¹) than for G2 (~ 3.9 kJ mol⁻¹).

Because both G2 and CBS-Q are composite computational

TABLE 3: Relative Energies of Mg(CN)₂ Isomers as a Function of Level of Theory^a

correlation basis	MP2				MP3			B3-LYP			
	6-31G*	6-31+G*	6-311G*	6-311+G*	6-31G*	6-31+G*	6-311G*	6-31G*	6-31+G*	6-311G*	6-311+G(2df)
CNMgNC	37.2	17.5	30.8	29.2	7.0	0	1.3	5.2	0	0	0
NCMgCN	0	0	0	0	0	13.4	0	0	9.2	3.2	9.8
NCMgNC	17.9	8.2	15.0	14.4	2.6	6.0	0.1	2.2	4.4	0.9	4.4
NCMg- π -(CN)	8.0	12.5	8.5	10.8	1.0	17.2	1.0	5.6	11.1		
CNMg- π -(CN)	25.5	20.2	23.0	25.5	3.7	10.2	1.0	8.3	9.2		
Mg- π -(CN) ₂	15.0	23.2	15.8	20.9	1.5	20.1	1.3	11.8	19.4		

^a Energies shown are in kJ mol⁻¹, do not include ZPE, and are expressed relative to the global minimum (CNMgNC or NCMgCN) at each level of theory. A space indicates that the species indicated is not a minimum at the relevant level of theory.

techniques, neither method is strictly variational. Thus, although the results presented in Table 1 suggest rather strongly that the global minimum is CNMgNC and that none of the π -complexes are genuine minima, these inferences are not conclusive. As noted above, it is questionable whether the MP2(full)/6-31G* basis set is sufficiently large to deliver highly accurate geometries for the various stationary points, and we address this matter more specifically in the next section.

Further Geometry Optimizations on Local Minima. In Table 3, we display relative energies for the various minima at different levels of theory; these results show that the precise shape of the potential energy surface is markedly level-dependent. Given the G2 and CBS-Q results discussed in the previous sections, this is not particularly surprising; nevertheless, there are some further points to note. First, at all levels of theory used here, the global minimum is one of two linear isomers, NCMgCN or CNMgNC; NCMgCN is favored in all of the MP2 optimizations and at MP3 and B3-LYP when diffuse functions are not included in the basis set. (The relative ordering of other isomers varies considerably, although the asymmetric linear isomer, NCMgNC, is always intermediate in energy between NCMgCN and CNMgNC.) Second, the π -complex geometries are found not to be stationary points in the B3-LYP calculations involving diffuse functions (6-31+G* and 6-311+G(2df)), although they can be located as local minima in all of the other MP2, MP3, and B3-LYP calculations included in Table 3; in the other B3-LYP calculations (using the 6-31G* and 6-311G* bases), the three π -complex geometries are higher in energy than any of the linear isomers. Third, the difference in energy between the highest and lowest energy isomers, at any level of theory, ranges from ~ 37 kJ mol⁻¹ (14 mhartree) for MP2(full)/6-31G* to only ~ 1.3 kJ mol⁻¹ (0.5 mhartree) for MP3(full)/6-311G*. The MP2 calculations display consistently larger energy ranges, between lowest and highest energy isomers, than do the MP3 or B3-LYP results.

Table 4 details the geometric parameters and low-frequency vibrational modes for each of these minima. There is little visible effect of basis set size upon bond length; considerably greater variation in bond length is seen for different correlation methods than for different basis sets, with MP2 optimizations yielding consistently longer C–N bonds than either MP3 or B3-LYP, while optimizations at B3-LYP furnish Mg–C and Mg–N bonds that are somewhat shorter than the MP2 or MP3 values. Good agreement is seen between MP2 and MP3 metal–ligand bond lengths and between MP3 and B3-LYP C–N distances. Previous studies have suggested that MP3 is generally superior to MP2 in predicting equilibrium geometries,¹⁹ while B3-LYP also yields much better bond lengths for several metal cyanide molecules than does MP2.^{5j,20} In this context, the agreement seen between MP3 and B3-LYP regarding C–N bond lengths is very encouraging. (The comparatively poor agreement between MP3 and B3-LYP values for the metal–ligand separa-

tions is arguably less significant, since these bonds are always characterized by lower force constants than the C–N bonds.)

The most variable parameters in these very floppy structures are the π -complex bond angles. A trend, consistent across all levels of theory surveyed, is for the optimized \angle (XMgN) and \angle (MgNC) angles to increase (for the same basis set) from MP2 to MP3 to B3-LYP; this includes also the tendency for \angle (MgNC) angles to collapse to 180° in the B3-LYP calculations when diffuse functions are included. Again, these results suggest (but do not prove) that the π -complex geometries are not true minima.

Potential Optimizations on NCMg- π -(CN). To study the potential energy surface around NCMg- π -(CN) in greater detail, we have relied most heavily on B3-LYP calculations to explore the effect of basis set size. This method was chosen in preference to any purely ab initio technique, both for reasons of reduced computational expense (MP2 optimizations using a large basis set become prohibitively expensive for a species such as Mg(CN)₂, featuring five heavy atoms) and for the presumed high accuracy of B3-LYP geometries obtained using a large basis set.^{5j,20} For example, a recent study on Mg(CN) isomerism has found near-perfect agreement between the experimental rotational constant B_0 and the same parameter calculated at the B3-LYP/6-311+G(3df) level for the MgNC isomer.²⁰ Agreement between the corresponding parameters for the other isomer, MgCN, is less striking; nevertheless, the calculations at B3-LYP/6-311+G(3df) are able, in each case, to yield rotational constants to within 1% of the experimental values, and the B3-LYP and experimental bond lengths for MgCN are also in agreement to within 1%.²⁰ While we have not attempted any geometry optimizations using a basis set as large as 6-311+G(3df), we have employed the 6-311+G(2df) basis in our B3-LYP calculations. As a check on the relative performance of these two basis sets, we have executed B3-LYP/6-311+G(2df) optimizations on MgCN and MgNC. The optimized geometries for these species feature C–N bond lengths that agree to within ± 0.0002 Å of the B3-LYP/6-311+G(3df) parameters,²⁰ while the Mg–C and Mg–N bond lengths are increased by only 0.004 Å when the smaller 6-311+G(2df) basis set is used. Furthermore, as discussed in the previous section, generally good agreement is seen between MP3 and B3-LYP geometry optimizations on the Mg(CN)₂ stationary points. We are thus confident that our best B3-LYP partially optimized geometries for the various bent conformations of NCMg(CN) provide a very accurate description of this portion of the minimum-energy pathway to isomerization between NCMgCN and NCMgNC. (This is not to say, however, that the presence or absence of a local minimum in the vicinity of NCMg- π -(CN) should be regarded as definitive; the best assessment of this matter will be by calculations involving a high level of correlation and a large basis set.)

As noted in the previous section, the B3-LYP calculations

TABLE 4: Structural Parameters for Mg(CN)₂ Isomers as a Function of Level of Theory^a

correlation basis	MP2				MP3			B3-LYP			
	6-31G*	6-31+G*	6-311G*	6-311+G*	6-31G*	6-31+G*	6-311G*	6-31G*	6-31+G*	6-311G*	6-311+G(2df)
CNMgNC											
<i>r</i> (N–Mg)	1.9209	1.9263	1.9218	1.9252	1.9134	1.9180	1.9134	1.9079	1.9154	1.9095	1.8992
<i>r</i> (C–N)	1.1952	1.1946	1.1900	1.1910	1.1816	1.1808	1.1762	1.1849	1.1839	1.1778	1.1736
ν_1, ν_2	65.7 (Π_u)	86.3 (Π_u)	57.4 (Π_u)		69.1 (Π_u)			62.4 (Π_u)	83.4 (Π_u)	66.8 (Π_u)	
NCMgCN											
<i>r</i> (C–Mg)	2.0407	2.0438	2.0392	2.0432	2.0401	2.0424	2.0389	2.0346	2.0391	2.0329	2.0292
<i>r</i> (N–C)	1.1870	1.1880	1.1814	1.1823	1.1654	1.1661	1.1596	1.1667	1.1674	1.1591	1.1559
ν_1, ν_2	75.6 (Π_u)	91.7 (Π_u)	75.8 (Π_u)		76.3 (Π_u)			72.7 (Π_u)	82.6 (Π_u)	77.3 (Π_u)	
NCMgNC											
<i>r</i> (C–Mg)	2.0368	2.0386	2.0357	2.0391	2.0372	2.0383	2.0366	2.0324	2.0358	2.0306	2.0270
<i>r</i> (Mg–N')	1.9224	1.9280	1.9242	1.9285	1.9133	1.9179	1.9142	1.9099	1.9177	1.9107	1.9008
<i>r</i> (N–C)	1.1868	1.1879	1.1812	1.1821	1.1654	1.1662	1.1595	1.1666	1.1674	1.1590	1.1558
<i>r</i> (N–C')	1.1952	1.1948	1.1899	1.1908	1.1818	1.1811	1.1762	1.1852	1.1843	1.1779	1.1737
ν_1, ν_2	70.0 (Π)	85.9 (Π)	63.7 (Π)		72.0 (Π)			65.0 (Π)	80.3 (Π)	71.2 (Π)	
NCMg- π -(CN)											
<i>r</i> (C–Mg)	2.0389	2.0428	2.0361	2.0404	2.0381	2.0409	2.0362	2.0328	NM ^b	2.0309	NM ^b
<i>r</i> (N–C)	1.1868	1.1882	1.1812	1.1821	1.1653	1.1663	1.1595	1.1665		1.1590	
<i>r</i> (Mg–C')	2.1790	2.2191	2.1871	2.1999	2.2540	2.3755	2.2541	2.3151		2.3130	
<i>r</i> (Mg–N')	2.0712	2.0511	2.0506	2.0478	2.0199	1.9802	2.0088	1.9914		1.9894	
<i>r</i> (N'–C')	1.2020	1.2030	1.1960	1.1967	1.1853	1.1869	1.1791	1.1874		1.1792	
\angle (MgN'C')	78.6°	81.5°	80.0°	80.8°	85.2°	93.8°	85.8°	89.8°		90.0°	
\angle (CMgN')	162.5°	164.0°	162.7°	163.3°	166.1°	169.3°	165.9°	168.2°		168.3°	
ν_1	89.4 (A')	90.9 (A')	94.2 (A')		90.0 (A')			86.6 (A')		86.7 (A')	
ν_2	94.4 (A'')	99.9 (A'')	98.5 (A'')		96.1 (A'')			94.4 (A'')		101.2 (A'')	
CNMg- π -(CN)											
<i>r</i> (N–Mg)	1.9205	1.9281	1.9220	1.9281	1.9124	1.9181	1.9125	1.9083	NM ^b	1.9097	NM ^b
<i>r</i> (C–N)	1.1953	1.1947	1.1899	1.1907	1.1817	1.1810	1.1761	1.1849		1.1777	
<i>r</i> (Mg–C')	2.1681	2.1989	2.1822	2.1941	2.2275	2.2970	2.2434	2.2902		2.2889	
<i>r</i> (Mg–N')	2.0719	2.0580	2.0495	2.0478	2.0287	2.0012	2.0107	1.9955		1.9947	
<i>r</i> (N'–X')	1.2022	1.2031	1.1963	1.1970	1.1852	1.1863	1.1790	1.1871		1.1791	
\angle (MgN'C')	78.0°	80.1°	79.8°	80.5°	83.3°	88.4°	85.2°	88.2°		88.3°	
\angle (NMgN')	161.5°	162.7°	162.5°	163.1°	164.3°	166.3°	165.3°	166.7°		166.8°	
ν_1	78.2 (A')	95.6 (A')	71.2 (A'')		81.3 (A')			73.2 (A')		78.4 (A')	
ν_2	78.6 (A'')	98.2 (A'')	72.0 (A')		82.1 (A'')			75.4 (A'')		83.3 (A'')	
Mg- π -(CN) ₂											
<i>r</i> (N–C)	1.2022	1.2032	1.1962	1.1969	1.1853	1.1864	1.1790	1.1872	NM ^b	1.1792	NM ^b
<i>r</i> (C–Mg)	2.1768	2.2100	2.1828	2.1940	2.2381	2.3127	2.2379	2.3040		2.3114	
<i>r</i> (N–Mg)	2.0676	2.0505	2.0493	2.0473	2.0228	1.9957	2.0112	1.9924		1.9869	
\angle (MgN'C')	78.6°	81.0°	79.8°	80.5°	84.2°	89.5°	84.8°	89.1°		90.1°	
\angle (NMgN')	153.8°	156.7°	155.3°	156.3°	158.6°	161.3°	159.2°	162.0°		162.4°	
\angle (CNMgN')	135.5°	134.2°	133.6	134.1°	134.2°	136.4°	131.9°	133.7°		133.8°	
ν_1	61.5 (A)	57.8 (A)	59.7 (A)		57.4 (A)			45.0 (A)		39.8 (A)	
ν_2	120.1 (B)	120.8 (B)	137.1 (B)		118.2 (B)			109.4 (B)		100.8 (A)	

^a Bond lengths in angstroms, bond angles in degrees, and vibrational frequencies (uncorrected) in cm⁻¹. Only the lowest one or two fundamental vibrational frequencies are given. ^b This species is not a minimum at the indicated level of theory.

employing diffuse functions do not locate any π -complex minima. Consequently, the B3-LYP potential energy curves for the 6-31+G* and 6-311+G(2df) basis sets do not feature any barrier to isomerization between NCMg- π -(CN) and NCMgNC, while the corresponding curves for 6-31G* and 6-311G* do indicate a small barrier. Nevertheless, all the B3-LYP calculations show that the potential energy surface in the vicinity of the putative minimum is very flat. A depiction of the B3-LYP results, for NCMg(CN), is given in Figure 4; it is apparent from this graph that the existence of the π -complex NCMg- π -(CN) is precarious at all of these levels of theory.

Further Single-Point Calculations. We have employed the B3-LYP/6-311+G(2df) partially optimized geometries detailed above, for points neighboring the putative minimum at NCMg- π -(CN), to investigate the curvature of the PES through various high-level single-point calculations. Levels of theory used in this analysis encompass MP2, MP4SDTQ, QCISD, QCISD(T), CCSD, and CCSD(T), using 6-31G and 6-311G basis sets with various polarization and diffuse functions. Figures 5–7 are indicative of the potential energy curves obtained. A

combination of level-dependent and basis-set-dependent features emerges from an analysis of the results.

(1) All methods show a tendency, in keeping with the trend noted above for B3-LYP calculations, for the isomerization barrier to diminish with inclusion of diffuse functions. This effect is most prominent for the 6-31G(d) basis, for which the addition of diffuse functions is seen to lower the barrier by between 50% and 95%; in contrast, diffuse functions are seen to reduce the barrier at 6-311G(d) or 6-311G(2df) by only about 20%. The barrier at 6-311+G(d) is somewhat larger than that at 6-31+G(d) for all methods.

(2) Increasing the number of polarization functions, from d to 2df for a 6-311G basis, reduces the barrier by between 50% and 85% for all methods. Further augmentation, from 2df to 3df, increases the barrier by a small amount (determined only for MP2).

(3) For all basis sets surveyed, the barrier height is largest at MP2 and smallest at QCISD and CCSD; this effect can be seen in Figure 7, which shows the potential energy curves generated using the 6-311+G(d) basis.

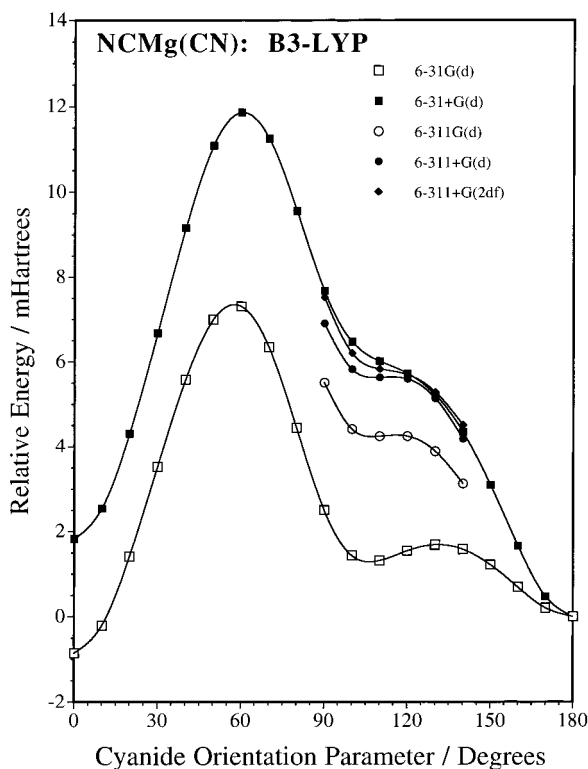


Figure 4. Potential energy curve depicting the minimum energy pathway connecting the isomerization processes $\text{NCMgCN} \leftrightarrow \text{NCMg-}\pi\text{(CN)}$ and $\text{NCMg-}\pi\text{(CN)} \leftrightarrow \text{NCMgNC}$, calculated using the B3-LYP hybrid density functional theory and employing basis sets ranging from 6-31G* to 6-311+G(2df). All energies depicted are expressed relative to NCMgNC at the same level of theory. The cyanide orientation parameter, which we have used to describe the partially optimized geometries, is defined as the angle subtended by the C atom (of the CN ligand undergoing rearrangement), the C–N bond midpoint, and the Mg atom; a value of 0° for this parameter therefore represents a linear MgCN moiety (and 180° indicates a linear MgNC fragment), while a value of 90° describes a structure in which the Mg is equidistant from the C and N atoms.

Barrier heights obtained using the largest basis sets, for each correlation method, are as summarized in Table 5. All methods find that a barrier to $\text{NCMg-}\pi\text{(CN)}$ isomerization does exist and yield a barrier height of less than 5 kJ mol^{-1} . Nevertheless, the range in barrier heights found in Table 5 is of 1 order of magnitude; further calculations, with larger basis sets than those employed here, would help to determine whether $\text{NCMg-}\pi\text{(CN)}$ has any real claim to stability. While such calculations are currently prohibitively demanding of our computational resources, they can satisfactorily be emulated in a number of ways. We have used the B3-LYP/6-311+G(2df) partially optimized geometries and the appropriate sequence of single-point total energy calculations to obtain G2 and CBS-Q values for various single points along the minimum energy pathway on the potential energy surface in the vicinity of $\text{NCMg-}\pi\text{(CN)}$. These results are depicted in Figure 8.

The $\text{NCMg-}\pi\text{(CN)}$ isomerization barrier, according to the “composite” methods of G2 and CBS-Q with B3-LYP/6-311+G(2df) partially optimized geometries, is only 0.12 mhartrees (0.32 kJ mol^{-1} , G2) or 0.04 mhartrees (0.11 kJ mol^{-1} , CBS-Q). The good agreement between these two techniques, which correspond to significantly higher levels of theory than any of the single-point total-energy calculations used to obtain the barrier heights in Table 5, is very gratifying. It should be noted, however, that none of these barrier heights have been adjusted for basis set superposition effects. We find that the

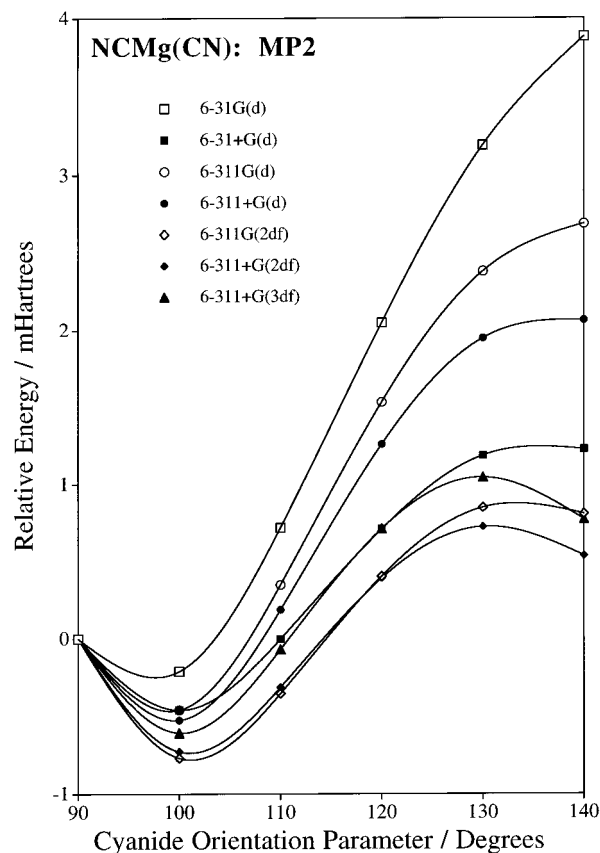


Figure 5. Potential energy curve, in the vicinity of the $\text{NCMg-}\pi\text{(CN)}$ putative minimum, obtained using single-point MP2(fc) total energies (with a variety of basis sets) from B3-LYP/6-311+G(2df) partially optimized geometries. Energies are expressed relative to the 90° partially optimized structure; the cyanide orientation parameter is as described in the caption to Figure 4. Note that the total range of the y-axis is approximately 13 kJ mol^{-1} .

counterpoise corrections²¹ for the G2 calculations act to reduce the isomerization barrier to only 0.02 mhartrees, in excellent agreement with the CBS-Q value (for which we have not attempted a counterpoise correction).

Discussion

The accord evident between B3-LYP/6-311+G(2df) calculations and G2 and CBS-Q calculations employing B3-LYP/6-311+G(2df) partially optimized geometries allows us to infer that the barrier to NCMgNC formation from $\text{NCMg-}\pi\text{(CN)}$ is exceedingly small and is almost certainly below 1 kJ mol^{-1} ; with such a small barrier, the lifetime of $\text{NCMg-}\pi\text{(CN)}$ would be negligible even within an argon matrix at a temperature of 20 K. While we have not attempted any such detailed analysis for the other π -complex structures, the G2 and CBS-Q values reported in Table 1 suggest that all of the π -complexes are of comparable stability; this supposition is supported by G2 explorations of the potential energy surface in the vicinities of $\text{NCMg-}\pi\text{(CN)}$, $\text{CNMg-}\pi\text{(CN)}$, and $\text{Mg-}\pi\text{(CN)}_2$ (employing partially optimized MP2/6-31G* geometries), indicating that all of these species have isomerization barriers of less than 1 kJ mol^{-1} . It therefore appears most unlikely that any Mg(CN)_2 π -complex geometries correspond to species of any real stability against isomerization. In contrast, the cyanide/isocyanide interconversion barriers (which are typically $\sim 20 \text{ kJ mol}^{-1}$ above the higher energy isomer, according to both G2 and CBS-Q calculations) are sufficiently robust to ensure that each of the linear isomers NCMgCN , NCMgNC , and CNMgNC can exist independently at low (but conveniently accessible) temperatures.

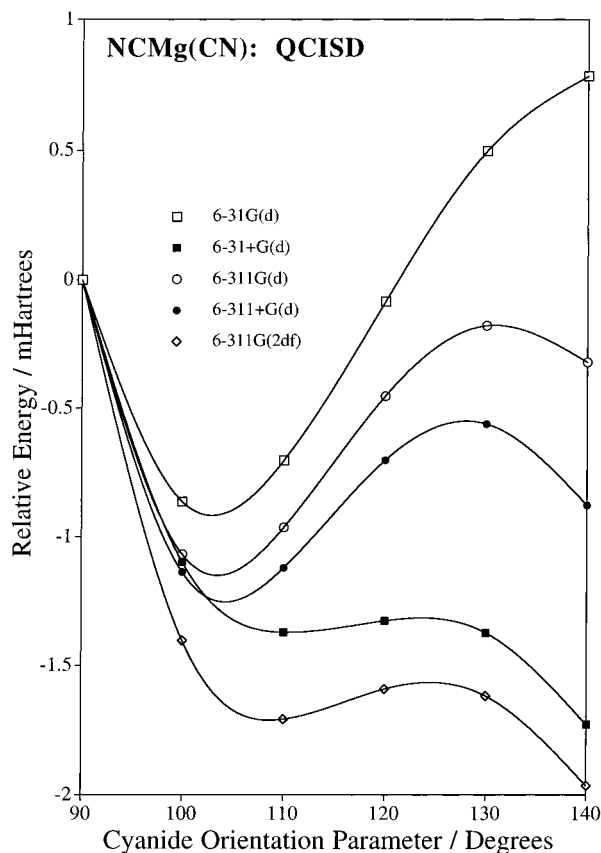


Figure 6. Potential energy curve, in the vicinity of the NCMg- π -(CN) putative minimum, obtained using single-point QCISD(fc) total energies (with a variety of basis sets) from B3-LYP/6-311+G(2df) partially optimized geometries. Energies are expressed relative to the 90° partially optimized structure; the cyanide orientation parameter is as described in the caption to Figure 4. Note that the total range of the y-axis is approximately 8 kJ mol⁻¹.

Why are the π -complexes not stable? Recall that Na(CN) possesses a π -complex global minimum, which is consistent with an essentially electrostatic Na⁺/CN⁻ interaction. Furthermore, the global minimum for Mg(CN)⁺, a species that is isoelectronic with Na(CN), is also a π -complex. If addition of a cyanide ligand to Mg²⁺ thus produces a π -complex, why is this π -bonding not preserved when a second cyanide ligand is added? The most reasonable explanation is that the metal–ligand bonding in Mg(CN)₂ is less perfectly ionic and contains a greater degree of covalent character than the bonding in either Na(CN) or Mg(CN)⁺. Some covalent character is certainly present in the Mg–CN configuration (within both NCMgCN and CN–MgCN), which displays rather more resistance to bending than is evident for the Mg–NC moiety; this can be appreciated upon examination of the shapes of the potential energy curves shown in Figure 4. There may well be a synergistic effect of sorts in which the coordination of two cyanide ligands to Mg²⁺ serves to reduce the effective positive charge upon the magnesium atom just sufficiently to destabilize the (more ionic) π -complex geometries relative to the (partially covalent) linear geometries NCMgCN, NCMgNC, and CNMgNC.

An interesting parallel may also be drawn with lithium cyanide, with which magnesium dicyanide shares a diagonal relationship. A π -complex local minimum for Li(CN) is also found at some levels of theory,⁵ but only the isocyanide LiNC has been observed spectroscopically. Both lithium and magnesium have electronegativities marginally above that of sodium so that the metal/cyanide interaction for Li and Mg is expected

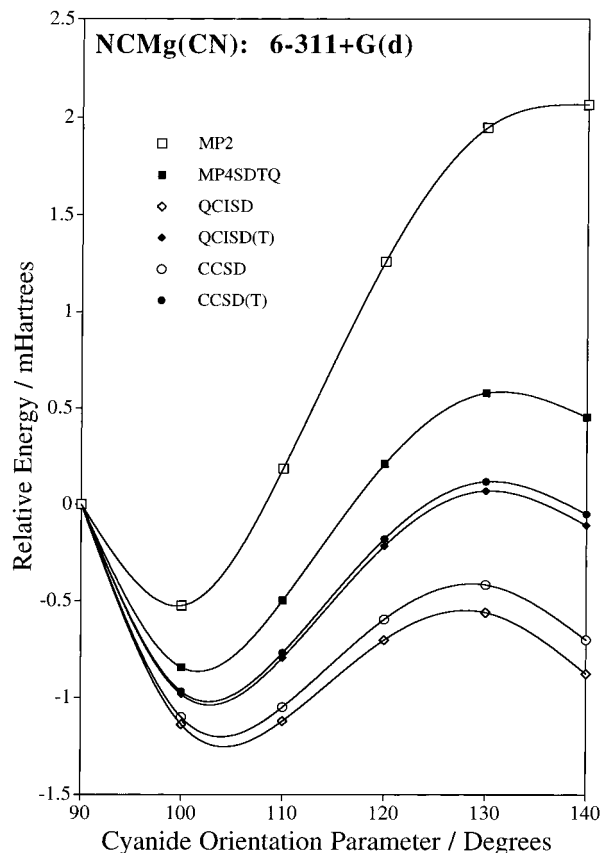


Figure 7. Potential energy curve, in the vicinity of the NCMg- π -(CN) putative minimum, obtained using single-point total energies (with a 6-311+G(d) basis set, and a variety of levels of correlation) for B3-LYP/6-311+G(2df) partially optimized geometries. Energies are expressed relative to the 90° partially optimized structure; the cyanide orientation parameter is as described in the caption to Figure 4. Note that the total range of the y-axis is approximately 10.5 kJ mol⁻¹.

TABLE 5: Barrier Heights to Isomerization of NCMg- π -(CN) as a Function of Level of Theory

method ^a	E_{rel}^b
MP2/6-311+G(3df)	1.65 (4.3)
MP4SDTQ/6-311G(2df)	0.54 (1.4)
QCISD/6-311G(2df)	0.15 (0.4)
QCISD(T)/6-311+G(d)	1.11 (2.9)
CCSD/6-311+G(d)	0.79 (2.1)
CCSD(T)/6-311+G(d)	1.14 (3.0)

^a Level of theory employed in single-point total energy calculations upon a series of partially optimized geometries (obtained using B3-LYP/6-311+G(2df)) in the vicinity of the putative minimum NCMg- π -(CN). ^b Energy of isomerization barrier, relative to the potential well corresponding to NCMg- π -(CN), in mhartrees (and kJ mol⁻¹, in brackets). Relative energies reported here do not include ZPE and have not been corrected for basis set superposition error (BSSE) effects.

to be slightly less polarized than is the case in Na(CN). In this context, it would appear valuable to reassess the larger alkaline earth dicyanides, which are found also to possess several π -complex minima at the levels of theory employed in Kapp and Schleyer's study.⁹ Do the potential energy surfaces for these species retain all of the π -coordinated geometries when examined at higher levels of theory?

It is useful also to reexamine the potential energy surfaces obtained for Mg(CN)₂ at HF/6-31G* and at MP2/6-31G*. Clearly (from the data in Table 1), both surfaces substantially overestimate the relative energy differences between isomers, yet it is Hartree–Fock and not second-order Møller–Plesset that gets the ordering of isomers correct. The HF/6-31G*

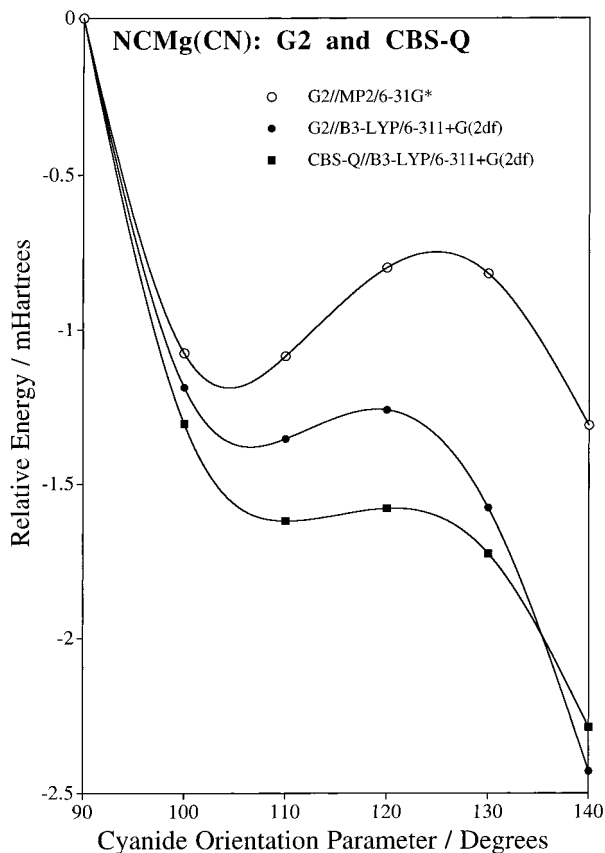


Figure 8. Potential energy curve, in the vicinity of the NCMg- π (CN) putative minimum, obtained by summation of the relevant single-point total energies to yield G2 and CBS-Q values for the B3-LYP/6-311+G(2df) partially optimized geometries. Energies are expressed relative to the 90° partially optimized structure; the cyanide orientation parameter is as described in the caption to Figure 4. The total range of the y-axis is approximately 6.5 kJ mol⁻¹.

calculations also determine, correctly (as far as we can tell!), that there are no stable “bent” geometries upon the potential energy surface, while MP2/6-31G* appears to be quite misleading on this point. This system thus represents one instance where, fortuitously, the single-electron HF method is seen to give a better result than is obtained with the inclusion of electron correlation (if only small basis sets are employed). Hartree–Fock calculations do not, however, reveal the feature that is more or less consistently found in all of the calculations using some form of correlation, namely, that the potential energy surface in the vicinity of any of the (unstable) π -complex geometries is remarkably flat, and this may well manifest itself as a large-amplitude bending motion of the Mg–NC moiety.

We recommend an experimental investigation of the isomerism of Mg(CN)₂, but note in passing that the microwave spectroscopy of Mg(CN)₂ may be rather disappointing; only one Mg(CN)₂ isomer, linear NCMgNC, is predicted to be both isolable and rotationally active!

Conclusions

The potential energy surface for Mg(CN)₂ isomerization is very flat, with G2 and CBS-Q calculations predicting an energy difference of only 30–35 kJ mol⁻¹ between the global minimum and the highest saddle point to interconversion. Many qualitative differences are evident between the results from different levels of theory. The highest-level calculations employed here (G2 and CBS-Q) determine CNMgNC to be the global minimum (in conflict with an earlier study, which assigned NCMgCN as

the lowest energy isomer), while calculations at these levels also overturn the findings, at lower levels, that π -complex geometries exist as stable minima. We find that the only discrete magnesium dicyanide species are the three linear isomers CNMgNC, CNMgCN, and NCMgCN.

Acknowledgment. The author thanks Eric A. Magnusson for helpful discussions. Thanks are also due to the Australian Research Council for a research block infrastructure grant for computer hardware and to the Australian Cooperative Supercomputer Facility for CPU time on the Australian National University’s Silicon Graphics Power Challenge supercomputer.

References and Notes

- (1) (a) Pearson, P. K.; Schaefer, H. F.; Wahlgren, U. *J. Chem. Phys.* **1975**, *65*, 350. (b) Pau, C. F.; Hehre, W. J. *J. Phys. Chem.* **1982**, *86*, 321. (c) Murrell, J. N.; Carter, S.; Halonen, L. O. *J. Mol. Spectrosc.* **1982**, *93*, 307. (d) Lee, T. J.; Rendell, A. P. *Chem. Phys. Lett.* **1991**, *177*, 491. (e) Bowman, J. M.; Gazdy, B.; Bentley, J. A.; Lee, T. J.; Dateo, C. E. *J. Chem. Phys.* **1993**, *99*, 308. (f) Rao, V. S.; Vijay, A.; Chandra, A. K. *Can. J. Chem.* **1996**, *74*, 1072.
- (2) (a) Klein, M. L.; Goddard, J. D.; Bounds, D. G. *J. Chem. Phys.* **1981**, *75*, 3909–15. (b) Marsden, C. J. *J. Chem. Phys.* **1982**, *76*, 6451. (c) Spoliti, M.; Ramondo, F.; Diomedes-Camassei, F.; Bencivenni, L. *J. Mol. Struct. (THEOCHEM)* **1994**, *312*, 41. (d) Makarewicz, J.; Ha, T. K. *J. Mol. Struct. (THEOCHEM)* **1994**, *315*, 149. (e) Dorigo, A.; Schleyer, P. von R.; Hobza, P. *J. Comput. Chem.* **1994**, *15*, 322. (f) Bouslama, L.; Daoudi, A.; Mestdagh, H.; Rolando, C.; Suard, M. *J. Mol. Struct. (THEOCHEM)* **1995**, *330*, 187. (g) Petrie, S. *J. Phys. Chem.* **1996**, *100*, 11581.
- (3) van Vaals, J. J.; Meerts, W. L.; Dymanus, A. *J. Chem. Phys.* **1982**, *77*, 5245–6.
- (4) See, for example: (a) Maruani, J.; Serre, J., Eds. *Symmetries and Properties of Non-Rigid Molecules: A Comprehensive Survey*; Elsevier: Amsterdam, 1983. (b) Smeyers, Y. G. *Structure and Dynamics of Non-Rigid Molecular Systems*; Kluwer: Dordrecht, 1984. (c) Farantos, S. C.; Tennyson, J. *J. Chem. Phys.* **1985**, *82*, 800. (d) Nefedova, V. V.; Boldyrev, A. I.; Simons, J. *J. Chem. Phys.* **1993**, *98*, 8801.
- (5) (a) Ismail, Z. K.; Hauge, R. H.; Margrave, J. L. *J. Chem. Phys.* **1972**, *57*, 5137. (b) Clementi, E.; Kistenmacher, H.; Popkie, H. *J. Chem. Phys.* **1973**, *58*, 2460. (c) Schmiedekamp, A.; Bock, C. W.; George, P. *J. Mol. Struct.* **1980**, *67*, 107. (d) Essers, R.; Tennyson, J.; Wormer, P. E. *S. Chem. Phys. Lett.* **1982**, *89*, 223. (e) Brocks, G.; Tennyson, J. *J. Mol. Spectrosc.* **1983**, *99*, 263. (f) Brocks, G.; Tennyson, J.; van der Avoird, A. *J. Chem. Phys.* **1984**, *80*, 3223. (g) Schleyer, P. v. R.; Sawaryn, A.; Reed, A. E.; Hobza, P. *J. Comput. Chem.* **1986**, *7*, 666. (h) Adamowicz, L.; Frum, C. I. *Chem. Phys. Lett.* **1989**, *157*, 496. (i) Wang, Y.; Hong, X.; Liu, J.; Wen, Z. *J. Mol. Struct. (THEOCHEM)* **1996**, *369*, 173. (j) Juršic, B. S. *J. Mol. Struct. (THEOCHEM)* **1998**, *428*, 41.
- (6) (a) Bauschlicher, C. W.; Langhoff, S. R.; Partridge, H. *Chem. Phys. Lett.* **1985**, *115*, 124. (b) Kawaguchi, K.; Kagi, E.; Hirano, T.; Takano, S.; Saito, S. *Astrophys. J.* **1993**, *406*, L39. (c) Anderson, M. A.; Steimle, T. C.; Ziurys, L. M. *Astrophys. J.* **1994**, *429*, L41. (d) Anderson, M. A.; Ziurys, L. M. *Chem. Phys. Lett.* **1994**, *231*, 164. (e) Ishii, K.; Hirano, T.; Nagashima, U.; Weis, B.; Yamashita, K. *J. Mol. Struct. (THEOCHEM)* **1994**, *305*, 117. (f) Barrientos, C.; Largo, A. *J. Mol. Struct. (THEOCHEM)* **1995**, *336*, 29. (g) Woon, D. E. *Astrophys. J.* **1996**, *456*, 602. (h) Petrie, S. *J. Chem. Soc., Faraday Trans.* **1996**, *92*, 1135–40. (i) Lanzisera, D. V.; Andrews, L. *J. Phys. Chem. A* **1997**, *101*, 9666. (j) Kieninger, M.; Irving, K.; Rivas-Silva, F.; Palma, A.; Ventura, O. N. *J. Mol. Struct. (THEOCHEM)* **1998**, *422*, 133.
- (7) (a) Kuijpers, P.; Törring, T.; Dymanus, A. *Chem. Phys. Lett.* **1976**, *42*, 423. (b) Törring, T.; Bekoooy, J. P.; Meerts, W. L.; Hoefl, J.; Tiemann, E.; Dymanus, A. *J. Chem. Phys.* **1980**, *73*, 4875. (c) Wormer, P. E. S.; Tennyson, J. *J. Chem. Phys.* **1981**, *75*, 1245. (d) Tennyson, J.; Sutcliffe, B. T. *J. Chem. Phys.* **1982**, *77*, 4061. (e) Van Vaals, J. J.; Meerts, W. L.; Dymanus, A. *J. Mol. Spectrosc.* **1984**, *106*, 280.
- (8) (a) Furio, N.; Dagdigian, P. *J. Chem. Phys. Lett.* **1985**, *115*, 358. (b) Ellingboe, L. C.; Boppegger, A. M. R. P.; Brazier, C. R.; Bernath, P. F. *Chem. Phys. Lett.* **1986**, *126*, 285. (c) Whitham, C. J.; Soep, B.; Visticot, J.-P.; Keller, A. *J. Chem. Phys.* **1990**, *93*, 991. (d) Steimle, T. C.; Fletcher, D. A.; Jung, K. Y.; Scurlock, C. T. *J. Chem. Phys.* **1992**, *97*, 2909; **1994**, *100*, 4025. (e) Scurlock, C. T.; Steimle, T. C.; Suenram, R. D.; Lovas, F. J. *J. Chem. Phys.* **1994**, *100*, 3497. (f) Scurlock, C. T.; Fletcher, D. A.; Steimle, T. C. *J. Chem. Phys.* **1994**, *101*, 7255. (g) Nanbu, S.; Minamino, S.; Aoyagi, M. *J. Chem. Phys.* **1997**, *106*, 8073.
- (9) Kapp, J.; Schleyer, P. von R. *Inorg. Chem.* **1996**, *35*, 2247.
- (10) Frisch, M. F.; Trucks, G. W.; Schlegel, H. B.; Gill, P. M. W.; Johnson, B. G.; Robb, M. A.; Cheeseman, J. R.; Keith, T.; Al-Laham, M. A.; Zakrzewski, V. G.; Ortiz, J. V.; Foresman, J. B.; Cioslowski, J.; Stefanov,

B. B.; Nanayakkara, A.; Challacombe, M.; Peng, C. Y.; Ayala, P. Y.; Chen, W.; Wong, M. W.; Andres, J. L.; Replogle, E. S.; Gomperts, R.; Martin, R. L.; Fox, D. J.; Binkley, J. S.; DeFrees, D. J.; Baker, J.; Stewart, J. J. P.; Head-Gordon, M.; Gonzalez, C.; Pople, J. A. *Gaussian94*, revision B.2; Gaussian, Inc.: Pittsburgh, PA, 1995.

(11) Curtiss, L. A.; Raghavachari, K.; Trucks, G. W.; Pople, J. A. *J. Chem. Phys.* **1991**, *94*, 7221.

(12) Curtiss, L. A.; Raghavachari, K.; Pople, J. A. *J. Chem. Phys.* **1995**, *103*, 4192.

(13) Ochterski, J. W.; Petersson, G. A.; Montgomery, J. A. *J. Chem. Phys.* **1996**, *104*, 2598.

(14) Curtiss, L. A.; Raghavachari, K.; Redfern, P. C.; Pople, J. A. *J. Chem. Phys.* **1997**, *106*, 1063.

(15) Curtiss, L. A.; Raghavachari, K.; Redfern, P. C.; Stefanov, B. B. *J. Chem. Phys.* **1998**, *108*, 692.

(16) More generally, the study by Kapp and Schleyer (ref 9) does not report any structures CNM- π -(CN) for M = Be, Mg, Ca, Sr, or Ba; since, for all alkaline earths except Be, the analogous structure NCM- π -(CN) is

found to be a minimum at the MP2(full)/6-31+G* level of theory, it would appear likely that CNM- π -(CN) is also a minimum (at moderate levels of theory) for M = Ca, Sr, and Ba.

(17) Scott, A. P.; Radom, L. *J. Phys. Chem.* **1996**, *100*, 16502.

(18) We have also determined standard¹³ CBS-Q total energies for the linear isomers NCMgCN, NCMgNC, and CNMgNC; these values are higher than those reported in Table 1 by 0.76, 0.67, and 0.74 mhartrees, respectively, with most of the difference attributable to variation in the ZPE at HF/6-31G* and at HF/6-311G**. Note that the influence (of the levels of theory chosen for geometry optimization and ZPE) on the CBS-Q relative energies of NCMgCN, NCMgNC, and CNMgNC is less than 0.1 mhartrees (<0.25 kJ mol⁻¹).

(19) DeFrees, D. J.; Raghavachari, K.; Schlegel, H. B.; Pople, J. A. *J. Am. Chem. Soc.* **1982**, *104*, 5576.

(20) Kieninger, M.; Irving, K.; Rivas-Silva, F.; Palma, A.; Ventura, O. N. *J. Mol. Struct. (THEOCHEM)* **1998**, *422*, 123.

(21) Boys, S. F.; Bernardi, F. *Mol. Phys.* **1970**, *19*, 553.